BEST AVAILABLE IMAGES

Defective images within this document are accurate representations of the original documents submitted by the applicant.

Defects in the images may include (but are not limited to):

- BLACK BORDERS
- TEXT CUT OFF AT TOP, BOTTOM OR SIDES
- FADED TEXT
- ILLEGIBLE TEXT
- SKEWED/SLANTED IMAGES
- COLORED PHOTOS
- BLACK OR VERY BLACK AND WHITE DARK PHOTOS
- GRAY SCALE DOCUMENTS

IMAGES ARE BEST AVAILABLE COPY.

As rescanning documents *will not* correct images, please do not report the images to the Image Problem Mailbox.

Intellectual Property Office
of New Zealand
Te Pou Rāhui Hanga Hou

CERTIFICATE

This certificate is issued in support of an application for Patent registration in a country outside New Zealand pursuant to the Patents Act 1953 and the Regulations thereunder.

I hereby certify that annexed is a true copy of the Provisional Specification as filed on 24 December 1998 with an application for Letters Patent number 333589 made by THOMAS PROFT, JOHN DAVID FRASER.

PRIORITY DOCUMENT
SUBMITTED OR TRANSMITTED IN COMPLIANCE WITH RULE 17.1(a) OR (b)

Dated 31 January 2000.

Neville Harris
Commissioner of Patents

Patents Form No. 4

PATENTS ACT 1953

PROVISIONAL SPECIFICATION

SUPERANTIGENS

333589

We, **JOHN DAVID FRASER**, C/- Auckland UniServices Limited, UniServices House, 58 Symonds Street, Auckland, New Zealand; and **THOMAS PROFT**, C/- Auckland UniServices Limited, UniServices House, 58 Symonds Street, Auckland, New Zealand, do hereby declare this invention to be described in the following statement:

(followed by page 1A)

SUPERANTIGENS

TECHNICAL FIELD

This invention relates to superantigens, and to their use, including in diagnosis and/or treatment of disease.

BACKGROUND ART

Bacterial superantigens are the most potent T cell mitogens known. They stimulate large numbers of T cells by directly binding to the side of the MHC class II and T cell Receptor (TcR) molecules. Because they override the normally exquisite MHC restriction phenomenon of T cell antigen recognition, they are prime candidates for either causing the onset of autoimmune diseases or exacerbating an existing autoimmune disorder.

The applicants have identified genes coding for four novel superantigens from *S. pyogenes*. It is broadly to these superantigens and polynucleotides encoding them that the present invention is directed.

SUMMARY OF THE INVENTION

In one aspect the invention provides a superantigen selected from any one of SMEZ-2, SPE-G, SPE-H and SPE-J, or a functionally equivalent variant thereof.

In a further aspect the invention provides a polynucleotide molecule comprising a sequence encoding a superantigen chosen from SMEZ-2, SPE-G, SPE-H, SPE-J, or a functionally equivalent variant thereof.

In another aspect of the invention there is provided a method of subtyping Streptococci on the basis of superantigen genotype comprising detection of the presence of any or all of the above four superantigens or the corresponding genes.

In a further aspect the invention provides a construct comprising any of the above superantigens (or superantigen variants) bound to a cell-targeting molecule.

In yet a further aspect, the invention provides a pharmaceutical composition for therapy or prophylaxis comprising a superantigen or superantigen variant as described above linked to cell targeting molecule.

Other aspects of the invention will be apparent from the description provided below.

DESCRIPTION OF DRAWINGS

While the invention is broadly defined above, it further includes embodiments of which the following description provides examples. It will also be better understood with reference to the following drawings:

Fig 1: Multiple alignment of superantigen protein sequences.

The protein sequence of mature toxins were aligned using the PileUp programme on the GCG package. Regions of high sequence identity are in black boxes. The boxes below the sequences indicate the structural elements of SPE-C, as determined from the crystal structure (Roussel et al 1997 Nat. Struct. Biol. 4 no8:635-43). Regions with highest homology correspond to the β4, β5, ∝4 and ∝5 regions in SPE-C. The clear box near the C-terminus represents a primary zinc binding motif, a common feature of all toxins shown. The arrows on top of the sequence alignment show the regions of sequence diversity between SMEZ and SMEZ-2.

Figure 2: The nucleotide sequence of the portion of the smez-2 gene coding the mature SMEZ-2 superantigen.

Figure 3: Gel electrophoresis of the purified recombinant toxins.

A. Two micrograms of purified recombinant toxin were run on a 12.5% SDS-polyacrylamide gel to show the purity of the preparations; B. Two micrograms of purified recombinant toxin were run on an isoelectric focusing gel (5.5% PAA, pH 5-8). The isoelectric point (IEP) of rSMEZ-2, rSPE-G and rSPE-H is similar and was estimated at pH 7-8. The IEP of rSMEZ was estimated at pH 6-6.5.

Figure 4: Stimulation of human T cells with recombinant toxins.

PBLs were isolated from human blood samples and incubated with varying concentrations of recombinant toxin. After 3d, 0.1 μCi [^{3}H]-thymidine was added and cells were incubated for another 24h, before harvested and counted on a gamma counter. O, unstimulated; ▲, rSMEZ; □, rSMEZ-2; ◆, rSPE-G; ◪, rSPE-H.

Figure 5: Jurkat cell assay

Jurkat cells (bearing a Vβ8 TcR) and LG-2 cells were mixed with varying concentrations of recombinant toxin and incubated for 24h, before SeI cells were added. After 1d, 0.1 μCi [^{3}H]-thymidine was added and cells were counted after another 24h. The Vβ8 targeting SEE was used as a positive control. The negative control was SEA. Both SMEZ and SMEZ-2 were potent stimulators of Jurkat cells, indicating their ability to specifically target Vβ8 bearing T cells. O, unstimulated; ▲, rSEA; □, rSEE; ◆, rSMEZ; ■, rSMEZ-2.

Figure 6: Zinc dependent binding of SMEZ-2 to LG-2 cells

LG-2 cells were incubated in duplicates with 1 ng of ^{125}I labelled rSMEZ-2 and increasing amounts of unlabeled toxin at 37°C for 1h, and then the cells were washed and counted.

O, incubation in media; ▲, incubation in media plus 1mM EDTA; □, incubation in media plus 1 mM EDTA, 2 mM $ZnCl_2$.

Figure 7: Scatchard analysis of SMEZ-2 binding to LG-2 cells

One nanogram ^{125}I-labeled rSMEZ-2 was incubated in duplicates with LG-2 cells and a 2-fold dilution series of cold toxin (10 μg to 10 pg). After 1h, cells were washed and counted. Scatchard plots were performed as described by Cunningham et al 1989 Science 243:1330-1336.

Figure 8: Summary of competitive binding experiments.

Efficiency of each labelled toxin to compete with a 10,000-fold molar excess of any other unlabeled toxin for binding to LG-2 cells. ☐ , no competition; ▨, 25% competition; ▨ , 50% competition; ▨ 75% competition; ■ , 100% competition. The results within the boxes are at the bottom right have previously been published (Li et al. 1997).

Figure 9: Competition binding study with SMEZ-2.

LG-2 cells were incubated in duplicates with 1 ng of ^{125}I-labeled rSMEZ-2 and increasing amounts of unlabeled rSMEZ-2, rSEA, rSEB, rTSST or rSPE-C. After 1h cells were washed and counted.
O, rSMEZ-2; ▲, rSEA; ☐, rSEB; ◹ rTSST; ◆, rSPE-C.

DESCRIPTION OF THE INVENTION

The focus of the invention is the identification of four novel superantigens (SPE-G, SPE-H, SPE-J and SMEZ-2) and the corresponding polynucleotides which encode them.

Figure 1 shows the amino acid sequences of the above four superantigens together with those of previously identified superantigens SMEZ, SPE-C and SEA.

Of the four superantigens SPE-G, SPE-H, SPE-J and SMEZ-2, the latter is of greatest interest.

The smez-2 gene which encodes SMEZ-2 was identified in an experiment designed to produce recombinant SMEZ protein from *S. pyogenes 2035* genomic DNA. A full length smez gene was isolated from the strain but the DNA sequence of the smez gene of strain 2035 showed nucleotide changes in 36 positions (or 5%) compared to smez from strain M1 (Fig. 1). The deduced protein sequences differed in 17 amino acid residues (or 8.1%). This difference establishes this as a new gene, smez-2, and the encoded protein as a new superantigen, SMEZ-2.

The most significant difference between SMEZ and SMEZ-2 is an exchanged pentapeptide sequence at position 96-100, where the EEPMS sequence of SMEZ is converted to KTSIL in SMEZ-2 (Fig. 1). A second difference is at position 111-112, where an RR dipeptide is exchanged for GK in SMEZ-2. The remaining 10 different residues are spread over almost the entire primary sequence.

Figure 2 shows the nucleotide sequence encoding mature SMEZ-2 and the deduced amino acid sequence.

The invention is of course not restricted to superantigens/polynucleotides having the specific sequences of Figures 1 and 2. Instead, functionally equivalent variants are contemplated.

The phrase "functionally equivalent variants" recognises that it is possible to vary the amino acid/nucleotide sequence of a protein while retaining substantially equivalent functionality. For example, a protein can be considered a functional equivalent of another protein for a specific function if the equivalent protein is immunologically cross-reactive with and has at least substantially the same function as the original protein. The equivalent can be, for example, a fragment of the protein, a fusion of the protein with another protein or carrier, or a fusion of a fragment which additional amino acids. For example, it is possible to substitute amino acids in a sequence with equivalent amino acids using conventional techniques. Groups of amino acids normally held to be equivalent are:

(a) Ala, Ser, Thr, Pro, Gly;
(b) Asn, Asp, Glu, Gln;
(c) His, Arg, Lys;
(d) Met, Leu, Ile, Val; and
(e) Phe, Tyr, Trp.

Equally, DNA sequences encoding a particular product can vary significantly simply due to the degeneracy of the nucleic acid code.

The probability of one sequence being functionally equivalent to another can be measured by the computer algorithms BLASTP (Altschul *et al* 1990 J Mol Biol

215:403-410) and FASTA (Pearson *et al* 1988 Proc Natl Acad Sci 85 2444-2448) for proteins and DNA respectively.

Identification of these superantigens and of their properties gives rise to a number of useful applications. A first such application is in the genotyping of organisms by reference to their superantigen profile.

An illustration of this is subtyping of strains of *S. pyogenes*.

One feature which has been observed is that all clones of *S. pyogenes* so far found to be positive for SMEZ express either SMEZ-1 or SMEZ-2 but not both. Thus they are mutually exclusive, which enables a rapid diagnostic test which tells whether an isolate or a patient sample is either SMEZ-1 +ve or SMEZ-2 +ve. This will assist in the typing of the isolate.

This general diagnostic approach is most simply achieved by providing a set or primers which amplify either all or a subset of superantigen genes and that generate gene specific fragments. This can be modified to provide a simple qualitative ELISA-strip type kit that detects biotin labelled PCR fragments amplified by the specific primers and hybridised to immobilised sequence specific probes. This has usefulness for screening patient tissue samples for the presence of superantigen producing streptococcal strains.

Another approach is to provide monoclonal antibodies to detect each of the streptococcal superantigens. An ELISA kit containing such antibodies would allow the screening of large numbers of streptococcal isolates. A kit such as this would be useful for agencies testing for patterns in streptococcal disease or food poisoning outbreaks.

Another potential diagnostic application of the superantigens of the invention is in the diagnosis of disease, such as Kawasaki Syndrome (KS).

KS is an acute multi-system vasculitis of unknown aetiology. It occurs world-wide but is most prevalent in Japan or in Japanese ancestry. It primarily affects infants

and the young up to the age of 16. It is an acute disease that without treatment, can be fatal. Primary clinical manifestations include

- Prolonged fever
- Bilateral non-exudative conjunctivitis
- Indurtation and erythema of the extremities
- Inflammation of the lips and oropharynx
- Polymorphous skin rash
- Cervical lymphoadenopathy
- In 15-25% of cases, coronary arterial lesions develop.

These indications are used as a primary diagnosis of KS.

In Japan and the US, KS has become one of the most common causes of acquired heart disease in children. Treatment involves the immediate intravenous administration of gamma globulin (IVGG) during the acute phase of the disease and this significantly reduces the level of coronary lesions.

There are two clear phases to the disease, an acute phase and a convalescent phase. The acute phase is marked by strong immune activation. Several reports have suggested that superantigens are involved and many attempts have been made to link the disease to infection with superantigen producing strains of Streptococcus pyogenes. Features of the acute phase of KS are the expansion of Vβ 2 and to a lesser extent Vβ8 bearing T cells and an increase of DR expression T cells (a hallmark of T cell activation).

Because SMEZ-2 stimulates both Vβ2 and Vβ8 bearing T cells, testing for SMEZ-2 production is potentially very useful in the diagnosis of KS.

In addition to diagnostic applications, another application of the superantigens is reliant upon their ability to bind to other cells.

One of the most important features of superantigens is that they bind a large number or T cell receptor molecules by binding to the Vβ domain. They are the most potent of all T cell mitogens and are therefore useful to recruit and activate T cells in a relatively non-specific fashion.

This ability enables the formation of constructs in which the superantigen (or at least the T-cell binding portion of it) is coupled to a cell-targeting molecule, particularly an antibody, more usually a monoclonal antibody.

When a monoclonal antibody that targets a specific cell surface antigen (such as a tumor specific antigen) is coupled to a superantigen in such a construct, this generates a reagent that on the one hand will bind specifically to the tumor cell, and on the other hand recruit and selectively active T cells for the purpose of killing the targeted cell.

Bi-specific constructs of this type have important applications in therapy (particularly cancer therapy) and may be prepared by means known to those skilled in art. For example SMEZ-2 may be coupled to a tumor specific monoclonal antibody. The constructs may be incorporated into conventional carriers for pharmaceutically-active proteins.

Various aspects of the invention will now be described with reference to the following experimental section, which is included for illustrative purposes.

EXAMPLE

Materials and Methods

Identification of novel SAGs

The novel superantigens were identified by searching the *S. pyogenes* M1 genome database at the University of Oklahoma (http://www.genome.ou.edu/strep.html) with highly conserved β5 and α4regions of streptococcal and staphylococcal superantigens, using a TBlastN search programme.

The open reading frames were defined by translating the DNA sequences around the matching regions and aligning the protein sequences to known superantigens using the computer programes Gap. Multiple alignments and dendrograms were performed with Lineup and Pileup. The FASTA programme was used for searching

the SwissProt (Amos Bairoch, Switzerland) and PIR (Protein Identification Resource, USA) protein databases.

The leader sequences of SPE-G and SPE-H were predicted using the SP Scan programme All computer programmes are part of the GCG package (version 8).

Cloning of smez, smez-2, spe-g and spe-h.

Fifty nanograms of *S.pyogenes* M1 (ATCC 700294) or *S.pyogenes* 2035 genomic DNA was used as a template to amplify the smez DNA fragment and the smez-2 DNA fragment, respectively, by PCR using the primers smez-fw (TGGGATCCTTAGAAGTAGATAATA) and smez-rev (AAGAATTCTTAGGAGTCAATTTC) and Taq Polymerase (Promega). The primers contain a terminal tag with the restriction enzyme recognition sequences BamHI and EcoRI, respectively. The amplified DNA fragment, encoding the mature protein without the leader sequence (Kamezawa et al, 1997 Infect. Immun. 65 no9:38281-33) was cloned into a T-tailed pBlueScript SKII vector (Stratagene).

Spe-g and spe-h were cloned in a similiar approach, using the primers spe-g-fw (CTGGATCCGATGAAAATTTAAAAGATTTAA) and spe-g-rev (AAGAATTCGGGGGGAGAATAG), and primers spe-h-fw (TTGGATCCAATTCTTATAATACAACC) and spe-h-rev (AAAAGCTTTTAGCTGATTGACAC), respectively.

The DNA sequences of the subcloned toxin genes were confirmed by the dideoxy chain termination method using a Licor automated DNA sequencer. As the DNA sequences from the genomic database are all unedited raw data, 3 subclones of every cloning experiment were analyzed to ensure that no Taq polymerase related mutations were introduced.

Expression and purification of rSMEZ, rSMEZ-2, rSPE-G and rSPE-H.

Subcloned smez, smez-2 and spe-g fragments were cut from pBlueScript SKII vectors, using restriction enzymes BamHI and EcoRI (LifeTech), and cloned into pGEX-2T expression vectors (Pharmacia). Due to an internal EcoRI restriction site within the spe-H gene, the pBlueScript:spe-h subclone was digested with BamHI

and HindIII and the spe-h fragment was cloned into a modified pGEX-2T vector that contains a HindIII 3'cloning site.

Recombinant SMEZ, rSMEZ-2 and rSPE-H were expressed in *E.coli* DH5α cells as glutathione-S-tranferase (GST) fusion proteins. Cultures were grown at 37° C and induced for 3-4 h after adding 0.2 mM isopropyl-β-D-thiogalactopyranoside (IPTG). GST - SPE-G fusion protein was expressed in cells grown at 28° C.

The GST fusion proteins were purified on glutathione agarose as described previously (Li et al, 1997) and the mature toxins were cleaved off from GST by trypsin digestion. All recombinant toxins, except rSMEZ, were further purified by two rounds of cation exchange chromatography using carboxy methyl sepharose (Pharmacia). The GST-SMEZ fusion protein was trypsin digested on the GSH-column and the flow through containing the SMEZ was collected.

Gel electrophoresis

All purified recombinant toxins were tested on a 12% SDS-polyacrylamide gel according the procedure of Laemmli. The isoelectric point of the recombinant toxins was determined by isoelectric focusing on a 5.5% polyacrylamide gel using ampholine pH 5-8 (Pharmacia Biotech). The gel was run for 90 min at 1 W constant power.

Toxin proliferation assay

Human peripheral blood lymphocytes (PBL) were purified from blood of a healthy donor by Histopaque Ficoll (Sigma) fractionation. The PBL were incubated in 96-well round bottom microtiter plates at 10^5 cells per well with RPMI-10 (RPMI with 10% fetal calf serum) containing varying dilutions of recombinant toxins. The dilution series was performed in 1:5 steps from a starting concentration of 10 ng/ml of toxin. Pipette tips were changed after each dilution step. After 3 days 0.1 μCi [^{3}H]thymidine was added to each well and cells were incubated for another 24 h. Cells were harvested and counted on a scintillation counter.

Mouse leukocytes were obtained from spleens of 5 different mouse strains (SJL, B10.M, B10/J, C3H and BALB/C). Splenocytes were washed in DMEM-10, counted

in 5% acetic acid and incubated on microtiter plates at 10^5 cells per well with DMEM-10 and toxins as described for human PBLs.

TcR Vβ analysis.

Vβ enrichment analysis was performed by anchored multiprimer amplification (Hudson et al, 1993, J exp Med 177:175-185). Human PBLs were incubated with 20 pg/ml of recombinant toxin at 10^6 cells/ml for 3 d. A two-fold volume expansion of the culture followed with medium containing 20 ng/ml IL-2. After another 24h, stimulated and resting cells were harvested and RNA was prepared using Trizol reagent (Life Tech). A 500 bp β-chain DNA probe was obtained by anchored multiprimer PCR as described previously (38), radiolabeled and hybridized to del (36) individual Vβs and a Cβ DNA region dot blotted on a Nylon membrane. The membrane was analysed on a Molecular Dynamics Storm Phosphor imager using ImageQuant software. Individual Vβs were expressed as a percentage of all the Vβs determined by hybridization to the Cβ probe.

Jurkat cell assay

Jurkat cells (a human T cell line) and LG-2 cells (a human B lymphoblastoid cell line, homozygous for HLA-DR1) were harvested in log phase and resuspended in RPMI-10. One hundred microliter of the cell suspension, containing $1x10^5$ Jurkat cells and $2x10^4$ LG-2 cells were mixed with 100 µl of varying dilutions of recombinant toxins on 96 well plates. After incubating overnight at 37° C, 100 µl aliquots were transfered onto a fresh plate and 100 µl ($1x10^4$) of SeI cells (IL-2 dependent murine T cell line) per well were added. After incubating for 24 h, 0.1 µCi [^{3}H]thymidine was added to each well and cells were incubated for another 24 h. Cells were harvested and counted on a scintillation counter. As a control, a dilution series of IL-2 was incubated with SeI cells.

Computer aided modelling of protein structures

Protein structures of SMEZ2, SPE-G and SPE-H were created on a Silicon Graphics computer using InsightII/Homology software. The superantigens SEA, SEB and SPE-C were used as reference proteins to determine structurally conserved regions (SCRs). Coordinate files for SEA (1ESF), for SEB (1SEB) and for SPE-C (1AN8) were downloaded from the Brookhaven Protein Database. The primary amino acid sequences of the reference proteins and SMEZ2, SPE-G and SPE-H, respectively,

were aligned and coordinates from superimposed SCR's were assigned to the model proteins. The loop regions between the SCRs were generated by random choice. MolScript software (PJ Kraulis, 1991, J App Critallography 24:946-50) was used for displaying the computer generated images.

Radiolabeling and LG-2 binding experiments

Recombinant toxin was radioiodinated by the chloramine T method as previously described (by Li et al. 1997). Labeled toxin was seperated from free iodine by size exclusion chromatography using Sephadex G25 (Pharmacia). LG2 cells were used for cell binding experiments, as described (Li et al. 1997). Briefly, cells were harvested, resuspended in RPMI-10 and mixed at 10^6 cells/ml with ^{125}I-tracer toxin (1 ng) and 0.0001 to 10 μg of unlabeled toxin and incubated at 37° C for 1 h. After washing with ice cold RPMI-1 the pelleted cells were analyzed in a gamma counter. For zinc binding assays the toxins were incubated in either RPMI-10 alone, in RPMI-10 with 1 mM EDTA or in RPMI-10 with 1mM EDTA, 2 mM $ZnCl_2$.

Scatchard analysis was performed as described by Cunningham et al. 1989.
For competitive binding studies, 1 ng of ^{125}I-tracer toxin (rSMEZ, rSMES-2, rSPE-G, rSPE-H, rSEA, rSPE-C, or rTSST) was incubated with 0.0001 to 10 μg of unlabeled toxin (rSMEZ, rSMES-2, rSPE-G, rSPE-H, rSEA, rSEB, rSPE-C, and rTSST) for 1h. For SEB inhibition studies, 20 ng of ^{125}I-rSEB was used as tracer and samples were incubated for 4h.

Results

Identification and sequence analysis of superantigens.

The Oklahoma University *Streptococcus pyogenes* M1 genome database is accessible via the internet and contains a collection of more than 300 DNA sequence contigs derived from a shot gun plasmid library of the complete *S. pyogenes* M1 genome. The currently available DNA sequences cover about 95% of the total genome.
We searched this database with a highly conserved superantigen peptide sequence, using a search program that screens the DNA database for peptide sequences in all 6 possible reading frames. We found 8 significant matches and predicted the open

reading frames (ORFs) by aligning translated DNA sequences to complete protein sequences of known SAgs.

Five matches gave complete ORFs with significant homology to streptococcal and staphylococcal superantigens. Three of these ORFs correlate to SPE-C, SSA and the recently described SMEZ (Kamezawa et al. 1997), respectively. The remaining two ORFs could not be correlated to any known protein in the SwissProt and PIR databases. We named these novel putative superantigen genes spe-g and spe-h.
One ORF could not be generated completely due to its location close to the end of a contig. The DNA sequence of the missing 5'-end is located on another contig, and individual contigs have yet to be be assembled in the database. However, the available sequence shows an ORF for the 137 COOH-terminal amino acid residues of a putative novel superantigen which could not be found in the existing protein databases. We named this so far incomplete gene spe-j.

In two cases a complete ORF could not be defined due to several out-of-frame mutations. Although DNA sequencing errors on the unedited DNA sequences can't be completely ruled out, the high frequency of inserts and deletions probably represent natural mutation events on pseudogenes, which are no longer used.

To produce recombinant proteins of SMEZ, SPE-G and SPE-H, individual genes (coding for the mature toxins without leader sequence) were amplified by PCR, and subcloned for DNA sequencing. Both, *Str. pyogenes* M1 and *Str. pyogenes* 2035 genomic DNA were used and individual toxin gene sequences compared between the two strains. The spe-h gene was isolated from M1 strain, but could not be amplified from strain 2035 genomic DNA suggesting a restricted strain specificity for this toxin. The spe-g gene was cloned from both M1 and 2035, and DNA sequence analysis of both genes showed no differences. The full length smez gene was isolated from both strains, but DNA sequence comparison revealed some striking differences. The smez gene of strain 2035 showed nucleotide changes in 36 positions (or 5%) compared to smez from strain M1 (Fig. 1). The deduced protein sequences differed in 17 amino acid residues (or 8.1%). This difference was sufficient to indicate a new gene. We named this gene smez-2, because it is 95% homologous to smez.

The most significant difference between SMEZ and SMEZ-2 is an exchanged pentapeptide sequence at position 96-100, where the EEPMS sequence of SMEZ is converted to KTSIL in SMEZ2 (Fig. 1). A second cluster is at position 111-112, where an RR dipeptide is exchanged for GK in SMEZ-2. The remaining 10 different residues are spread over almost the entire primary sequence.

A revised superantigen family tree, based on primary amino acid sequence homology now shows 3 general subfamilies; group A comprises SPE-C, SPE-J, SPE-G, SMEZ and SMEZ-2, group B comprises SEC1-3, SEB, SSA, SPE-A and SEG and group C comprises SEA, SEE, SED, SEH and SEI. Two superantigens, TSST and SPE-H do not belong to any one of those subfamilies.

SMEZ, SMEZ-2, SPE-G and SPE-J are most closely related to SPE-C, increasing the number of this subfamily from 2 to 5 members. SPE-G shows the highest protein sequence homology with SPE-C (38.4% identity and 46.6% similarity). The homology of SPE-J to SPE-C is even more significant (56% identity and 62% similarity), but this comparison is only preliminary due to the missing NH_2-terminal sequence. SMEZ shows 30.9% / 40.7% homology to SPE-C and SMEZ-2 is 92% / 93% homologous to SMEZ.

SPE-H builds a new branch in the family tree and is most closely related to SED, showing 25% identity and 37.3% similarity.

Multiple alignment of SAg protein sequences (Fig. 1) shows that similarities are clustered within structure determining regions, represented by $\alpha 4$, $\alpha 5$, $\beta 4$ and $\beta 5$ regions. This applies to all toxins of the superantigen family (data not shown) and explains why superantigens like SPE-C and SEA have very similar overall structures despite their rather low sequence identity of 24.4 %.

Although SPE-H is less related to SPE-C it shows 2 common features with the "SPE-C subfamily": (I) a truncated NH_2-terminus, lacking the $\alpha 1$ region and (II) a primary zinc binding motif (H-X-D) at the C-terminus (Fig. 1). It has been shown for several superantigens that this motif is involved in a zinc coordinated binding to the β-chain of HLA-DR1.

Fusion proteins of GST-SMEZ, GST-SMEZ-2 and GST-SPE-H were completely soluble and gave yields of about 30 mg per liter. The GST-SPE-G fusion was insoluble when grown at 37° C, but mostly soluble when expressed in cells growing at 28° C. Although soluble GST-SPE-G yields were 20-30 mg per liter, solubility decreased after cleavage of the fusion protein with trypsin. Soluble rSPE-G was achieved by diluting the GST-SPE-G to less than 0.2 mg/ml prior to cleavage. After cation exchange chromatography, purified rSPE-G could be stored at about 0.4 mg/ml.

Recombinant SMEZ could not be separated from GST by ion exchange chromatography. Isoelectric focusing revealed that the isoelectric points of the two proteins are too similar to allow separation (data not shown). Therefore, rSMEZ was released from GST by cleaving with trypsin while still bound to the GSH agarose column. Recombinant SMEZ was collected with the flow through.

The purified recombinant toxins were applied to SDS-PAGE and isoelectric focusing (Fig. 3). Each toxin ran as a single band on the SDS PAA gel confirming their purity and their calculated molecular weights of 24.33 (SMEZ), 24.15 (SMEZ-2), 24.63 (SPE-G) and 23.63 (SPE-H) (Fig. 3A). The isoelectric focusing gel (Fig. 3B) shows a significant difference between rSMEZ and rSMEZ-2. Like most other staphylococcal and streptococcal toxins, rSMEZ-2 possesses a slightly basic isoelectric point at pH 7-8, but rSMEZ is acidic with an IEP at pH 6-6.5.

T cell proliferation and Vβ specificity

To ensure the native conformation of the purified recombinant toxins, a standard [^{3}H]thymidine incorporation assay was performed to test for their potency to stimulate peripheral blood lymphocytes (PBLs). All toxins were active on human T cells (Fig. 4). Recombinant SEA, rSEB, rSPE-C and rTSST were included as reference proteins. The mitogenic potency of these toxins was lower than described previously, but is regarded as a more accurate figure. In previous studies performed by us, a higher starting concentration of toxin (100 ng/ml) was used and tips were not changed in between dilutions. This led to significant carryover across the whole dilution range. In this study, the starting concentration was 10 ng/ml and tips were changed in between dilutions preventing any carryover.

The half maximal response for rSPE-G and rSPE-H was 2 pg/ml and 50 pg/ml, respectively. No activity was detected at less than 0.02 pg/ml and 0.1 pg/ml, respectively. Both toxins are therefore less potent than rSPE-C. Recombinant SMEZ was similar in potency to rSPE-C, with a $P_{50\%}$ value of 0.08 pg/ml and no detectable proliferation at less than 0.5 fg/ml. Recombinant SMEZ-2 showed the strongest mitogenic potency of all toxins tested or, as far as we are aware of, described elsewhere. The $P_{50\%}$ value was determined at 0.02 pg/ml and rSMEZ-2 was still active at less than 0.1 pg/ml. All $P_{50\%}$ values are summarized in Table 1.

TABLE 1

POTENCY OF RECOMBINANT TOXINS ON HUMAN AND MOUSE T CELLS.

	PROLIFERATION POTENTIAL $P_{50\%}$ [pg/ml]					
TOXIN	HUMAN	SJL	B10.M	B10/J	C3H	BALB/C
SEA	0.1	20	12	1.8	19	1000
SEE	0.2	10	12	1.5	50	15
SEB	0.8	7000	80,000	5000	10,000	1000
TSST	0.2	20	1000	1.2	100	10
SPE-C	0.1	>100,000	>100,000	>100,000	>100,000	>100,000
SMEZ	0.08	80	80	100	9000	200
SMEZ-2	0.02	100	15	10	800	18
SPE-G	2	>100,000	>100,000	>100,000	>100,000	>100,000
SPE-H	50	15	800	5000	100	1000

Human PBLs and mouse T cells were stimulated with varying amounts of recombinant toxin. The $P_{50\%}$ value reflects the concentration of recombinant toxin required to induce 50% maximal cell proliferation. No proliferation was detected for rSPE-C and rSPE-G at any concentration tested on murine T cells.

Murine T cells from 5 different mouse strains were tested for their mitogenic response to rSMEZ, rSMEZ-2, rSPE-G and rSPE-H (Table 1). Recombinant SPE-G showed no activity against any of the mouse strains tested. Recombinant SPE-H, rSMEZ and rSMEZ-2 showed varied potency depending on the individual mouse strain. For example, rSMEZ-2 was 500-fold more potent than rSPE-H in the B10/J strain, while rSPE-H was 7.5-fold more active than rSMEZ-2 in the SJL strain.

The most consistently potent toxin on murine T cells was rSMEZ-2 with $P_{50\%}$ values of 10 pg/ml in B10/J and 800 pg/ml in C3H. Recombinant SMEZ varied between 80 pg/ml in SJL and B10.M and 9000 pg/ml in C3H. The $P_{50\%}$ value for rSPE-H was between 15 pg/ml in SJL and 5000 pg/ml in B10/J.

TABLE 2

Vβ SPECIFICITY OF RECOMBINANT TOXINS ON HUMAN PBLS.

	PERCENT Vβ ENRICHMENT				
Vβ	Resting	SMEZ	SMEZ-2	SPE-G	SPE-H
1.1	0.2	0.3	0.4	1.2	1
2.1	0.4	8.4	1	17.9	8.6
3.2	4.8	3.1	2.5	3	2.4
4.1	3.5	24.8	14.4	11.2	5.2
5.1	6.2	1.4	2.5	5.7	2.2
5.3	5.6	2.2	4.1	4.7	4.1
6.3	3	0.8	2.3	4.7	3.5
6.4	5.4	2.1	5.9	9.6	5.6
6.9	6.9	3.5	9.3	19.1	12.2
7.3	3.5	15.3	7.3	3.2	12.6
7.4	9	13.5	11.7	2.9	6.3
8.1	8.7	20.7	36	4.5	2.4
9.1	0.3	0.05	0	1.2	2.3
12.3	0.8	1.6	2	3.2	2.6
12.5	3	1.2	2	3	2.3
15.1	0.6	0.5	0.7	1.2	0.8
23.1	0.2	0.1	0.3	0.8	1
total	62.1	99.7	102.8	97.1	75.2

Human PBLs were incubated with 20 pg/ml of recombinant toxin for 4d. Relative enrichment of Vβ cDNAs was analyzed from RNA of stimulated and reting PBLs by anchored primer PCR and reverse dot blot to a panel of 17 different Vβ cDNAs.

The values representing the highest Vβ enrichment are underlined.

The human TcR Vβ specificity of the recombinant toxins was determined by multiprimer anchored PCR and dot blot analysis using a panel of 17 human Vβ DNA regions. The Vβ enrichment after stimulation with toxin was compared to the Vβ profile of unstimulated PBLs (Table 2). The sum total of all Vβs stimulated by rSMEZ, rSMEZ-2 and rSPE-G was close to 100 % suggesting that the Vβs used in the panel represent all the targeted Vβs. On the other hand, the total of the Vβs stimulated by rSPE-H was only 75%. It is therefore likely that rSPE-H also stimulated some less common Vβs, which are not represented in the panel. The most dramatic response was seen with all toxins, except rSMEZ2, on Vβ2.1 bearing T cells (21-fold for rSMEZ, 45-fold for rSPE-G and 22-fold for rSPE-H). In contrast, rSMEZ2 gave only a 2.5-fold increase of Vβ2.1 T-cells. SPE-G also targeted Vβ4.1, Vβ6.9, Vβ9.1 and Vβ12.3 (3-4 fold). A moderate enrichment of Vβ12.6, Vβ9.1 and Vβ23.1 (4-8 fold) was observed with rSPE-H. Both, rSMEZ and rSMEZ2, targeted Vβ4.1 and Vβ8.1 with similiar efficiency (3-7-fold). This finding is of particular interest, because Vβ8.1 activity had been found in some, but not all *Str. pyogenes* culture supernatants and in crude preparations of SPE-A and SPE-C. Moreover, SPE-B has often been claimed to have Vβ8 specific activity, but has since been shown to be a contaminant previously called SpeX. The ability of rSMEZ and rSMEZ-2 to stimulate the Vβ8.1 Jurkat cell line was tested (Fig. 5) Recombinant SMEZ was less potent than the control toxin (rSEE), showing a half maximal response of 0.2 ng/ml, compared to 0.08 ng/ml with rSEE, but rSMEZ-2 was more potent than rSEE (0.02 ng/ml). No proliferation activity was observed with the negative control toxin rSEA.

MHC class II binding

To determine if there were significant structural differences, the protein structures of SMEZ-2, SPE-G and SPE-H were modelled onto the superimposed structurally conserved regions of SEA, SEB and SPE-C. The models showed that in all three proteins, the 2 amino acid side chains of the COOH-terminal primary zinc binding motif are in close proximity to a third potential zinc ligand to build a zinc binding site, similar to the zinc binding site observed in SEA and SPE-C.

The zinc binding residues in SPE-C are H167, H201, D203, and it is thought that H81 from the HLA-DR1 β-chain binds to the same zinc cation to form a regular tetrahedral complex. The two ligands of the primary zinc binding motif, H201 and

D203, are located on the β12 strand, which is part of the β-grasp motif, a common structural domain of superantigens. The third ligand, H167, comes from the β10 strand (Roussel et al. 1997).

In the model of SPE-G three potential zinc binding ligands (H167, H202 and D204) are located at corresponding positions. In the SMEZ-2 and the SPE-H models, the two corresponding β12 residues are H202, D204 and H198, D200, respectively. The third ligand in SPE-H (D160) and in SMEZ-2 (H162) comes from the β9 strand and is most similar to H187 in SEA. It has been shown from crystal structures that H167 of SPE-C and H187 of SEA are spatially and geometrically equivalent sites (Scad et al. 1997, Embo J 14 no 14:3292-301; Roussel et al. 1997).

All superantigens examined so far, except SPE-C, bind to a conserved motif in the MHC class II α1-domain. In SEB and TSST, hydrophobic residues on the loop between the β1 and β2 strand project into a hydrophobic depression in the MHCII α1-domain. This loop region has changed its character in SPE-C, where the hydrophobic residues (F44, L45, Y46 and F47 in SEB) are substituted by the less hydrophobic residues T33, T34 and H35. A comparison of this region on the computer generated models revealed that the generic HLA-DR1 α-chain binding site might also be missing. As the loop regions are generated by random choice, no conclusions can be made from their conformation in the models. However, in none of the three models does the β1-β2-loop have the required hydrophobic features observed in SEB and TSST Swaminathan, S. *et al., Nature* 359, No. 6398:801-6 (1992), Acharya *et al., Nature* 367, No. 6458: 94-7 (1994). The residues are I25, D26, F27, K28, T29 and S30 in SMEZ-2, T31, T32, N33, S34 in SPE-G and K28, N29, S30, P31, D32, I33, V34 and T35 in SPE-H.

SMEZ-2 differs from SMEZ in only 17 amino acids. In the model of SMEZ-2 with the position of those 17 residues, most of the exchanges are located on loop regions, most significantly on the β5-β6 loop with 5 consecutive residues replaced. The potential zinc binding site and the β1-β2 loop are not affected by the replaced amino acids.

The TcR Vβ specificity differs between SMEZ and SMEZ-2 by one Vβ. SMEZ strongly stimulates Vβ2 T cells, but SMEZ-2 does not (Table 2). One or more of the 17

exchanged residues in SMEZ/SMEZ-2 might therefore be directly involved in TcR binding. The exact position of the TcR binding site can not be predicted from the model as several regions have been implicated in TcR binding for different toxins. Crystal structures of SEC2 and SEC3, complexed with a TcR β-chain indicated the direct role of several residues located on α2, the β2-β3 loop, the β4-β5 loop and α4 (Fields et al. 1996 Nature 384 no 6605:188-92). On the other hand, binding of TSST to the TcR involves residues from α4, the β7-β8 loop and the α4-β9 loop (Acharya et al. 1994, Nature 367 no 6548:94-7). The SMEZ-2 model shows 3 residues, which might contribute to TcR binding. In SMEZ, Lys is exchanged for Glu at position 80 and Thr is exchanged for Ile at position 84, both on the β4-β5 loop. On the COOH-terminal end of the α4 helix, Ala is replaced by Ser at position 143.

The results from the computer modelled protein structures suggest that all 4 toxins, SMEZ, SMEZ-2, SPE-G and SPE-H, might bind to the HLA-DR1 β-chain in a zinc dependent fashion, similar to SEA and SPE-C, but might not be able to interact with the HLA-DR1 α-site, a situation that has so far only been observed with SPE-C (Roussel et al. 1997; Li et al. 1997).

To find out whether or not zinc is required for binding of the toxins to MHC class II, a binding assay was performed using human LG-2 cells (which are MHC class II expressing cells homozygous for HLA-DR1). Direct binding of ^{125}I-labeled toxins was completely abolished in the presence of 1 mM EDTA (Fig. 6, Table 3). When 2 mM $ZnCl_2$ was added, binding to the LG-2 cells could be restored completely. These results show that the toxins bind in a zinc dependent mode, most likely to the HLA-DR1 β-chain similar to SEA and SPE-C. However, it does yet not exclude the possibility of an additional binding to the HLA-DR1 α-chain.

TABLE 3

BINDING AFFINITIES AND ZINC DEPENDENCIES FOR SUPERANTIGENS TO HUMAN CLASS II

TOXIN	MHC CLASS II BINDING kd [nM]	ZINC DEPENDENCY
SEA	36/1000	++
SEB	340	-
TSST	130	-
SPE-C	70	++
SMEZ	65/1000	++
SMEZ-2	25/1000	++
SPE-G	16/1000	++
SPE-H	37/2000	++

The binding affinities of the toxins to MHC class II were determined by Scatchard analysis using LG-2 cells. Zinc dependency was determined by binding of recombinant toxins to LG-2 cells in the presence and absence of EDTA, as described in the Materials and Methods section.

The biphasic binding of SEA to HLA-DR1 can be deduced from Scatchard analysis. It shows that SEA possesses a high affinity binding site of 36 nM (which is the zinc dependent β-chain binding site) and a low affinity binding site of 1 μM (α-chain binding site). On the other hand, only one binding site for HLA-DR1 was deduced from Scatchard analysis with SEB, TSST and SPE-C, respectively (Table 3).

Therefore, Scatchard analysis was performed with radiolabeled rSMEZ, rSMEZ-2, rSPE-G and rSPE-H using LG-2 cells. All four toxins showed multiphasic curves with at least 2 binding sites on LG-2 cells, a high affinity site of 15-65 nM and a low affinity site of 1-2 μM (Fig. 7, Table 3).

In a further attempt to determine the orientation of the toxins on MHC class II competition binding experiments were performed. The recombinant toxins and reference toxins (rSEA, rSEB, rSPE-C and rTSST) were radiolabeled and tested with excess of unlabeled toxin for binding to LG-2 cells. The results are summarized in Fig. 8. Both, rSEA and rSPE-C, inhibited binding of labeled rSMEZ, rSMEZ-2, rSPE-G and rSPE-H, respectively. However, rSPE-C only partially inhibited binding (50%) of the labeled rSMEZ-2 (Fig. 9). Recombinant SEB did not compete with any other toxin, even at the highest concentration tested. Recombinant TSST was only slightly competitive against ^{125}I-labeled rSMEZ, rSMEZ-2 and rSPE-G, respectively, and did not inhibit rSPE-H binding at all.

Reciprocal competition experiments were performed. Recombinant SMEZ, rSMEZ-2 and rSPE-H prevented ^{125}I-rSEA from binding to LG-2 cells. However, only partial competition (50%) was observed even at the highest toxin concentrations (10,000 fold molar excess). Recombinant SPE-G did not prevent binding of ^{125}I-rSEA and ^{125}I-rTSST binding was only partially inhibited by rSMEZ, rSMEZ-2 and rSPE-H, but not by rSPE-G. Significantly, none of the toxins inhibited ^{125}I-rSEB binding, even at the highest concentration tested.

In a further set of competition binding experiments, rSMEZ, rSMEZ-2, rSPE-G and rSPE-H were tested for competition against each other. Both, rSMEZ and rSMEZ-2 competed equally with each other and also prevented binding of labeled rSPE-G and rSPE-H. In contrast, rSPE-G and rSPE-H did not inhibit any other toxin binding suggesting that these toxins had the most restricted subset of MHC class II molecules, which represent specific receptors.

The foregoing examples are illustrations of the invention. The invention may be carried out with the numerous variations and modifications as will be apparent to those skilled in the art. For example, a native superantigen may be replaced by a synthetic superantigen with on or more deletions, insertions and/or substitutions relative to the corresponding natural superantigen, provided that the superantigen activity is retained. Likewise there are many variations in the way in which the invention can be used in other aspects of it.

REFERENCES

Marrack, P., and J. Kappler. 1990. The staphylococcal enterotoxins and their relatives. *Science* 248:705-711.

Huber, B.T., P.N. Hsu, and N. Sutkowski. 1996. Virus-encoded superantigens. *Microbiol. Rev.* 60, no. 3:473-82.

Alouf, J.E., H. Knoell, and W. Koehler. 1991. The family of mitogenic, shock-inducing and superantigenic toxins from staphylococci and streptococci. Sourcebook of bacterial protein toxins., eds. J.E. Alouf and J.H. Freer. Academic Press, San Diego. 367-414 pp.

Betley, M.J., D.W. Borst, and L.B. Regassa. 1992. Staphylococcal enterotoxins, toxic shock syndrome toxin and streptococcal exotoxins: a comparative study of their molecular biology. *Chem. Immunol.* 55:1-35.

Ren, K., J.D. Bannan, V. Pancholi, A.L. Cheung, J.C. Robbins, V.A. Fischetti, and J.B. Zabriskie. 1994. Characterization and biological properties of a new staphylococcal exotoxin. *J. Exp. Med.* 180, no. 5:1675-83.

Munson, S.H., M.T. Tremaine, M.J. Betley, and R.A. Welch. 1998. Identification and Characterization Of Staphylococcal Enterotoxin Types G and I From Staphylococcus Aureus. *Infect. Immun.* 66, no. 7:3337-3348.

Herman, A., J.W. Kappler, P. Marrack, and A.M. Pullen. 1991. Superantigens: mechanism of T-cell stimulation and role in immune responses. *Annu. Rev. Immunol.* 9:745-772.

Janeway, C.J., J. Yagi, P.J. Conrad, M.E. Katz, B. Jones, S. Vroegop, and S. Buxser. 1989. T-cell responses to Mls and to bacterial proteins that mimic its behavior. *Immunol. Rev.* 107:61-68.

Fast, D.J., P.M. Schlievert, and R.D. Nelson. 1989. Toxic shock syndrome-associated staphylococcal and streptococcal pyrogenic toxins are potent inducers of tumor necrosis factor production. *Infect. Immun.* 57, no. 1:291-4.

Kotzin, B.L., D.Y. Leung, J. Kappler, and P. Marrack. 1993. Superantigens and their potential role in human disease. *Adv. Immunol.* 54, no. 99:99-166.

Bohach, G.A., D.J. Fast, R.D. Nelson, and P.M. Schlievert. 1990. Staphylococcal and streptococcal pyrogenic toxins involved in toxic shock syndrome and related illnesses. *Crit. Rev. Microbiol.* 17, no. 4:251-72.

Weeks, C.R., and J.J. Ferretti. 1986. Nucleotide Sequence of the Type A Streptococcal Exotoxin (Erythrogenic Toxin) Gene from *Streptococcus pyogenes* Bacteriophage T12. *Infect. Immun.* 52:144-150.

Goshorn, S.C., G.A. Bohach, and P.M. Schlievert. 1988. Cloning and characterization of the gene, speC, for pyrogenic exotoxin type C from Streptococcus pyogenes. *Mol. Gen. Genet.* 212, no. 1:66-70.

Mollick, J.A., G.G. Miller, J.M. Musser, R.G. Cook, D. Grossman, and R.R. Rich. 1993. A novel superantigen isolated from pathogenic strains of Streptococcus pyogenes with aminoterminal homology to staphylococcal enterotoxins B and C. *J. Clin. Invest.* 92, no. 2:710-9.

Van Den Busche, R.A., J.D. Lyon, and G.A. Bohach. 1993. Molecular evolution of the staphylococcal and streptococcal pyrogenic toxin gene family. *Mol. Phylogenet. Evol.* 2:281-292.

Dellabona, P., J. Peccoud, J. Kappler, P. Marrack, C. Benoist, and D. Mathis. 1990. Superantigens interact with MHC class II molecules outside of the antigen groove. *Cell* 62, no. 6:1115-21.

Fraser, J.D. 1989. High-affinity binding of staphylococcal enterotoxins A and B to HLA-DR. *Nature* 339, no. 6221:221-3.

Fleischer, B., and H. Schrezenmeier. 1988. T cell stimulation by staphylococcal enterotoxins. Clonally variable response and requirement for major histocompatibility complex class II molecules on accessory or target cells. *J. Exp. Med.* 167, no. 5:1697-707.

Mollick, J.A., R.G. Cook, and R.R. Rich. 1989. Class II MHC molecules are specific receptors for staphylococcus enterotoxin A. *Science* 244, no. 4906:817-20.

Schad, E.M., I. Zaitseva, V.N. Zaitsev, M. Dohlsten, T. Kalland, P.M. Schlievert, D.H. Ohlendorf, and L.A. Svensson. 1995. Crystal structure of the superantigen staphylococcal enterotoxin type A. *EMBO J.* 14, no. 14:3292-301.

Swaminathan, S., W. Furey, J. Pletcher, and M. Sax. 1992. Crystal structure of staphylococcal enterotoxin B, a superantigen. *Nature* 359, no. 6398:801-6.

Papageorgiou, A.C., K.R. Acharya, R. Shapiro, E.F. Passalacqua, R.D. Brehm, and H.S. Tranter. 1995. Crystal structure of the superantigen enterotoxin C2 from Staphylococcus aureus reveals a zinc-binding site. *Structure* 3, no. 8:769-79.

Sundstrom, M., L. Abrahmsen, P. Antonsson, K. Mehindate, W. Mourad, and M. Dohlsten. 1996. The crystal structure of staphylococcal enterotoxin type D reveals Zn2+-mediated homodimerization. *EMBO J.* 15, no. 24:6832-40.

Acharya, K.R., E.F. Passalacqua, E.Y. Jones, K. Harlos, D.I. Stuart, R.D. Brehm, and H.S. Tranter. 1994. Structural basis of superantigen action inferred from crystal structure of toxic-shock syndrome toxin-1. *Nature* 367, no. 6458:94-7.

Roussel, A., B.F. Anderson, H.M. Baker, J.D. Fraser, and E.N. Baker. 1997. Crystal structure of the streptococcal superantigen SPE-C: dimerization and zinc binding suggest a novel mode of interaction with MHC class II molecules. *Nat. Struct. Biol.* 4, no. 8:635-43.

Kim, J., R.G. Urban, J.L. Strominger, and D.C. Wiley. 1994. Toxic shock syndrome toxin-1 complexed with a class II major histocompatibility molecule HLA-DR1. *Science* 266, no. 5192:1870-4.

Hurley, J.M., R. Shimonkevitz, A. Hanagan, K. Enney, E. Boen, S. Malmstrom, B.L. Kotzin, and M. Matsumura. 1995. Identification of class II major histocompatibility complex and T cell receptor binding sites in the superantigen toxic shock syndrome toxin 1. *J. Exp. Med.* 181, no. 6:2229-35.

Seth, A., L.J. Stern, T.H. Ottenhoff, I. Engel, M.J. Owen, J.R. Lamb, R.D. Klausner, and D.C. Wiley. 1994. Binary and ternary complexes between T-cell receptor, class II MHC and superantigen in vitro. *Source (Bibliographic Citation): Nature* 369, no. 6478:324-7.

Li, P.L., R.E. Tiedemann, S.L. Moffat, and J.D. Fraser. 1997. The superantigen streptococcal pyrogenic exotoxin C (SPE-C) exhibits a novel mode of action. *J. Exp. Med.* 186, no. 3:375-83.

Hudson, K.R., R.E. Tiedemann, R.G. Urban, S.C. Lowe, J.L. Strominger, and J.D. Fraser. 1995. Staphylococcal enterotoxin A has two cooperative binding sites on major histocompatibility complex class II. *J. Exp. Med.* 182, no. 3:711-20.

Kozono, H., D. Parker, J. White, P. Marrack, and J. Kappler. 1995. Multiple binding sites for bacterial superantigens on soluble class II MHC molecules. *Immunity* 3, no. 2:187-96.

Tiedemann, R.E., and J.D. Fraser. 1996. Cross-linking of MHC class II molecules by staphylococcal enterotoxin A is essential for antigen-presenting cell and T cell activation. *J. Immunol.* 157, no. 9:3958-66.

Braun, M.A., D. Gerlach, U.F. Hartwig, J.H. Ozegowski, F. Romagne, S. Carrel, W. Kohler, and B. Fleischer. 1993. Stimulation of human T cells by streptococcal "superantigen" erythrogenic toxins (scarlet fever toxins). *J. Immunol.* 150, no. 6:2457-66.

Kline, J.B., and C.M. Collins. 1997. Analysis of the interaction between the bacterial superantigen streptococcal pyrogenic exotoxin A (SpeA) and the human T-cell receptor. *Mol. Microbiol.* 24, no. 1:191-202.

Fleischer, B., A. Necker, C. Leget, B. Malissen, and F. Romagne. 1996. Reactivity of mouse T-cell hybridomas expressing human Vbeta gene segments with staphylococcal and streptococcal superantigens. *Infect. Immun.* 64, no. 3:987-94.

Toyosaki, T., T. Yoshioka, Y. Tsuruta, T. Yutsudo, M. Iwasaki, and R. Suzuki. 1996. Definition of the mitogenic factor (MF) as a novel streptococcal superantigen that is different from streptococcal pyrogenic exotoxins A, B, and C. *Eur. J. Immunol.* 26, no. 11:2693-701.

Kamezawa, Y., T. Nakahara, S. Nakano, Y. Abe, J. Nozaki-Renard, and T. Isono. 1997. Streptococcal mitogenic exotoxin Z, a novel acidic superantigenic toxin produced by a T1 strain of Streptococcus pyogenes. *Infect. Immun.* 65, no. 9:3828-33.

Hudson, K.R., H. Robinson, and J.D. Fraser. 1993. Two adjacent residues in Staphylococcal enterotoxins A an E determine Tcell receptor V beta specificity. *J. Exp. Med.* 177:175-185.

Kraulis, P.J. 1991. MOLSCRIPT": a program to produce both detailed and schematic plots of protein structures. *J. Appl. Critallography* 24:946-950.

Cunningham, B.C., P. Jhurani, P. Ng, and J.A. Wells. 1989. Receptor and Antibody epitopes in human growth hormone identified by homologue scanning mutagenesis. *Science* 243:1330-1336.

Fields, B.A., E.L. Malchiodi, H. Li, X. Ysern, C.V. Stauffacher, P.M. Schlievert, K. Karjalainen, and R.A. Mariuzza. 1996. Crystal structure of a T-cell receptor beta-chain complexed with a superantigen [see comments]. *Nature* 384, no. 6605:188-92.

Wen, R., G.A. Cole, S. Surman, M.A. Blackman, and D.L. Woodland. 1996. Major histocompatibility complex class II-associated peptides control the presentation of bacterial superantigens to T cells. *J. Exp. Med.* 183, no. 3:1083-92.

Thibodeau, J., I. Cloutier, P.M. Lavoie, N. Labrecque, W. Mourad, T. Jardetzky, and R.P. Sekaly. 1994. Subsets of HLA-DR1 molecules defined by SEB and TSST-1 binding. *Science* 266, no. 5192:1874-8.

Abe, J., B.L. Kotzin, K. Jujo, M.E. Melish, M.P. Glode, T. Kohsaka, and D.Y. Leung. 1992. Selective expansion of T cells expressing T-cell receptor variable regions V beta 2 and V beta 8 in Kawasaki disease. *PNAS* 89, no. 9:4066-70.

Kawasaki, T. 1967. Acute febrile mucocutaneous syndrome with lymphoid involvement with specific desquamation of the fingers and toes in children. *Jpn. J. Allergol.* 16:178.

Leung, D.Y., R.C. Giorno, L.V. Kazemi, P.A. Flynn, and J.B. Busse. 1995. Evidence for superantigen involvement in cardiovascular injury due to Kawasaki syndrome. *J. Immunol.* 155, no. 10:5018-21.

Cockerill, F.R., R.L. Thompson, J.M. Musser, P.M. Schlievert, J. Talbot, K.E. Holley, W.S. Harmsen, D.M. Ilstrup, P.C. Kohner, M.H. Kim, B. Frankfort, J.M. Manahan, J.M. Steckelberg, F. Roberson, and W.R. Wilson. 1998. Molecular, Serological, and Clinical Features Of 16 Consecutive Cases Of Invasive Streptococcal Disease. *Clin. Infect. Dis.* 26, no. 6:1448-1458.

Kapur, V., K.B. Reda, L.L. Li, L.J. Ho, R.R. Rich, and J.M. Musser. 1994. Characterization and distribution of insertion sequence IS1239 in Streptococcus pyogenes. *Gene* 150, no. 1:135-40.

RUSSELL McVEAGH WEST WALKER

per
ATTORNEYS FOR THE APPLICANT

333589

FIG 1

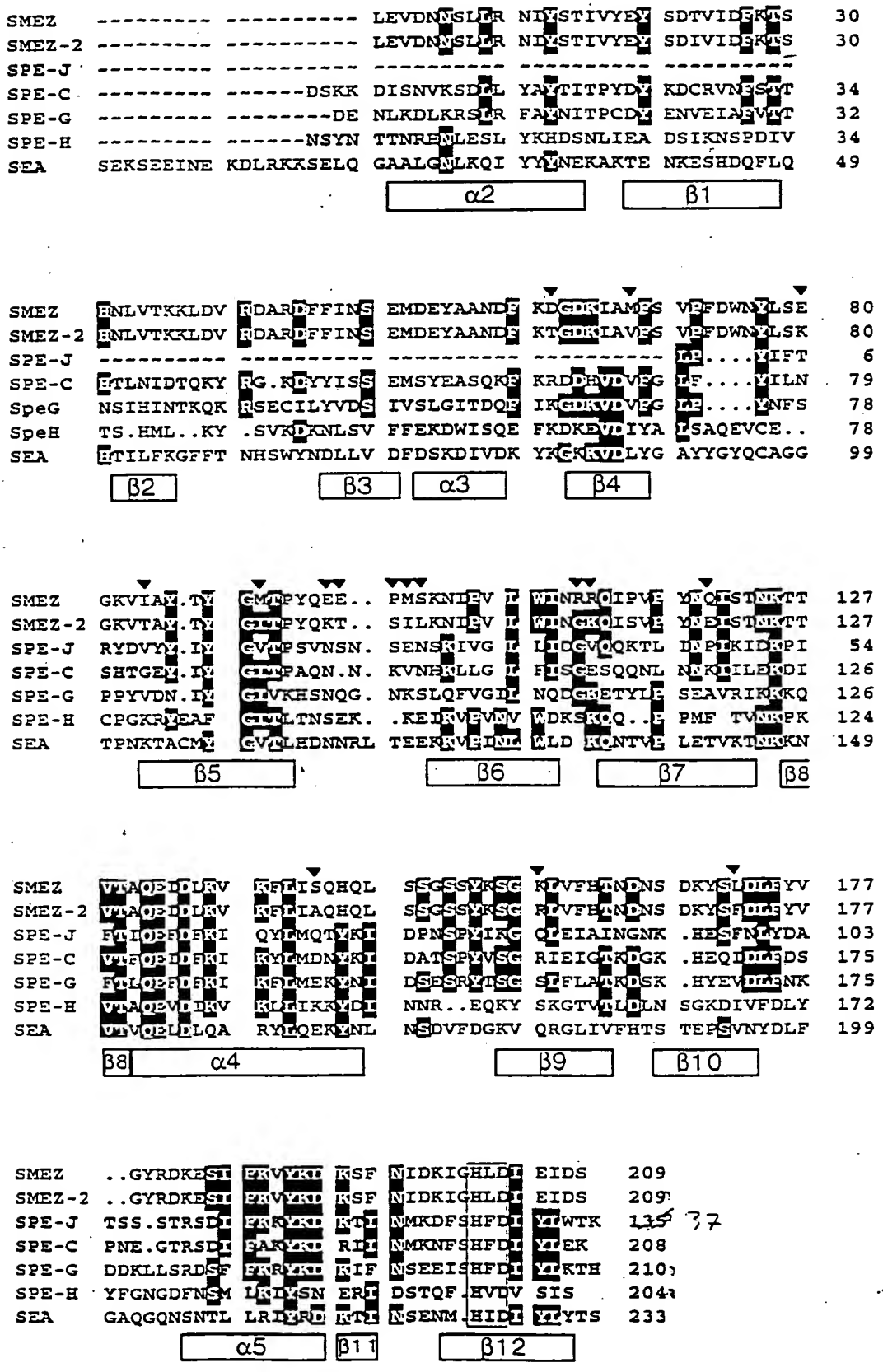
SMEZ
SMEZ-2
SPE-J
SPE-C
SPE-G
SPE-H
SEA
SpeG
SpeH
α2
β1
β2
β3
α3
β4
β5
β6
β7
β8
α4
β9
β10
α5
β11
β12

FIG. 2

```
                10                  30                  50
ATGAAAAAAACAAAACTTATTTTTTCTTTTACTTCAATATTCATTGCAATAATTTCTCGT
M  K  K  T  K  L  I  F  S  F  T  S  I  F  I  A  I  I  S  R

                70                  90                 110
CCTGTGTTTGGATTAGAAGTAGATAATAATTCCCTTCTAAGGAATATCTATAGTACGATT
P  V  F  G  L  E  V  D  N  N  S  L  L  R  N  I  Y  S  T  I

               130                 150                 170
GTATATGAATATTCAGATATAGTAATTGATTTTAAAACCAGTCATAACTTAGTGACTAAG
V  Y  E  Y  S  D  I  V  I  D  F  K  T  S  H  N  L  V  T  K

               190                 210                 230
AAACTTGATGTTAGAGATGCTAGAGATTTCTTTATTAACTCCGAAATGGACGAATATGCA
K  L  D  V  R  D  A  R  D  F  F  I  N  S  E  M  D  E  Y  A

               250                 270                 290
GCCAATGATTTTAAAACTGGAGATAAAATAGCTGTGTTCTCCGTCCCATTTGATTGGAAC
A  N  D  F  K  T  G  D  K  I  A  V  F  S  V  P  F  D  W  N

               310                 330                 350
TATTTATCAAAAGGAAAAGTCACAGCATATACCTATGGTGGAATAACACCCTACCAAAAA
Y  L  S  K  G  K  V  T  A  Y  T  Y  G  G  I  T  P  Y  Q  K

               370                 390                 410
ACTTCAATACCTAAAAAtatCCCTGTTAATTTATGGattaatGgAAAGcagatCTCTgtT
T  S  I  P  K  N  I  P  V  N  L  W  I  N  G  K  Q  I  S  V

               430                 450                 470
CcTtaCaaCGAAATATCaaCTAACAAAACAacaGTTACAGCTCAAGAAAttgATCTAAAG
P  Y  N  E  I  S  T  N  K  T  T  V  T  A  Q  E  I  D  L  K

               490                 510                 530
GTTAGAAAATTTTTAATAGCACAACATCAATTATATTCTTCTGGTTCTAGCTACAAAAGT
V  R  K  F  L  I  A  Q  H  Q  L  Y  S  S  G  S  S  Y  K  S

               550                 570                 590
GGTAGACTGGTTTTTCATACAAATGATAATTCAGATAAATATTCTTTCgatcTTTTctat
G  R  L  V  F  H  T  N  D  N  S  D  K  Y  S  F  D  L  F  Y

               610                 630                 650
gtagGATATAGAGATAAAGAAAGTATCTTTAAAGTATACAAAGACAATAAATCTTTCAAT
V  G  Y  R  D  K  E  S  I  F  K  V  Y  K  D  N  K  S  F  N

               670                 690
ATAGATAAAATTGGGCATTTAGATATAGAAATTGACTCCTAA
I  D  K  I  G  H  L  D  I  E  I  D  S  *
```

FIG 3

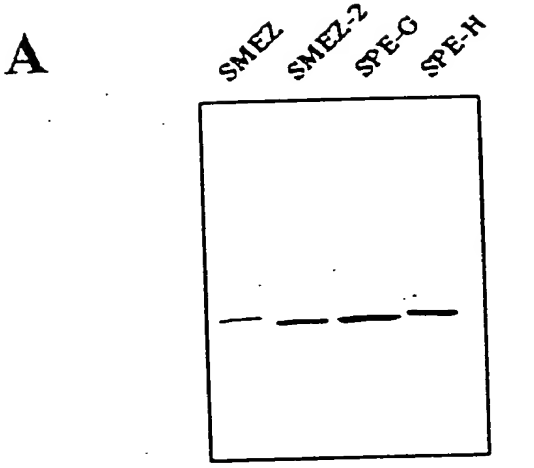

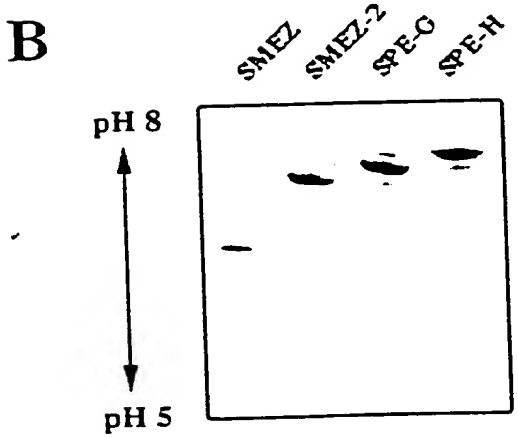

FIG 4

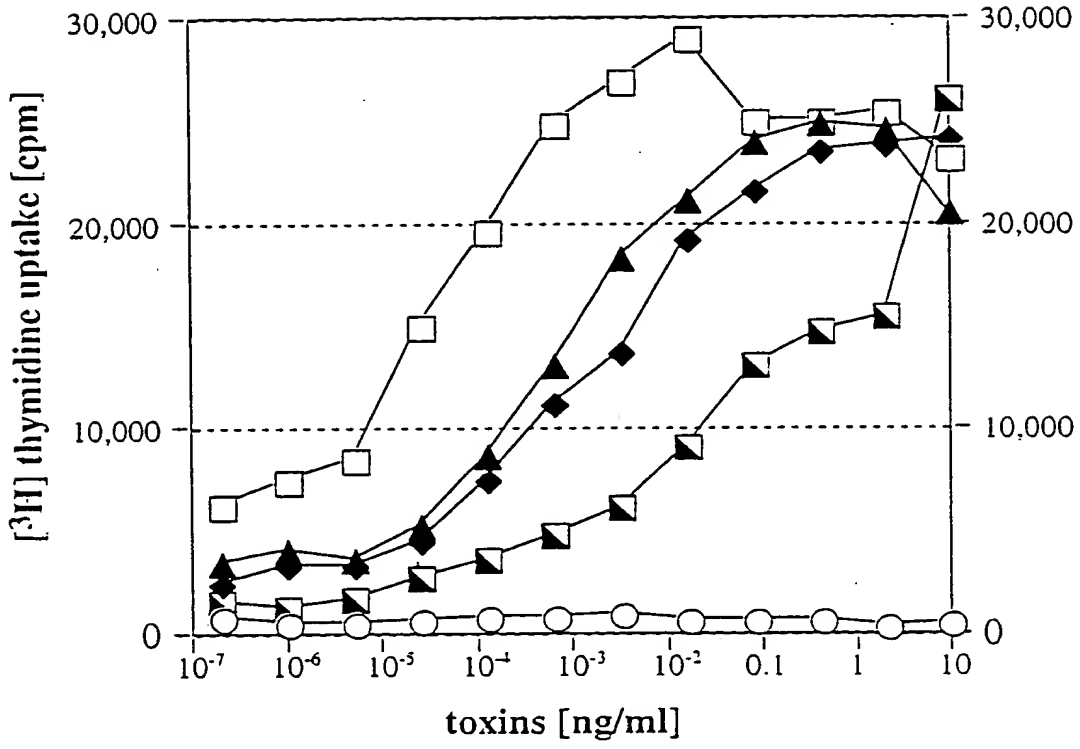
30,000
20,000
10,000
0
[3H] thymidine uptake [cpm]
10-7
10-6
10-5
10-4
10-3
10-2
0.1
1
10
toxins [ng/ml]

FIG 5

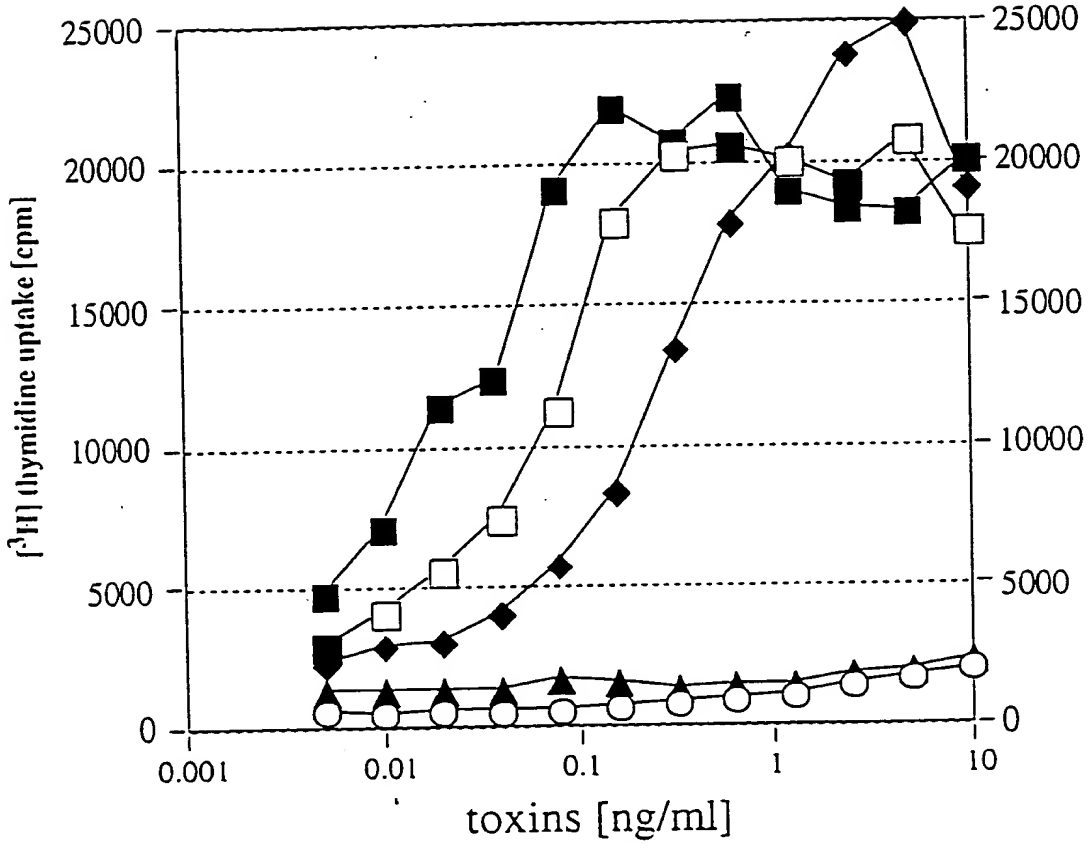
25000
20000
15000
10000
5000
0
[3H] thymidine uptake [cpm]
0.001
0.01
0.1
1
10
toxins [ng/ml]

FIG 6

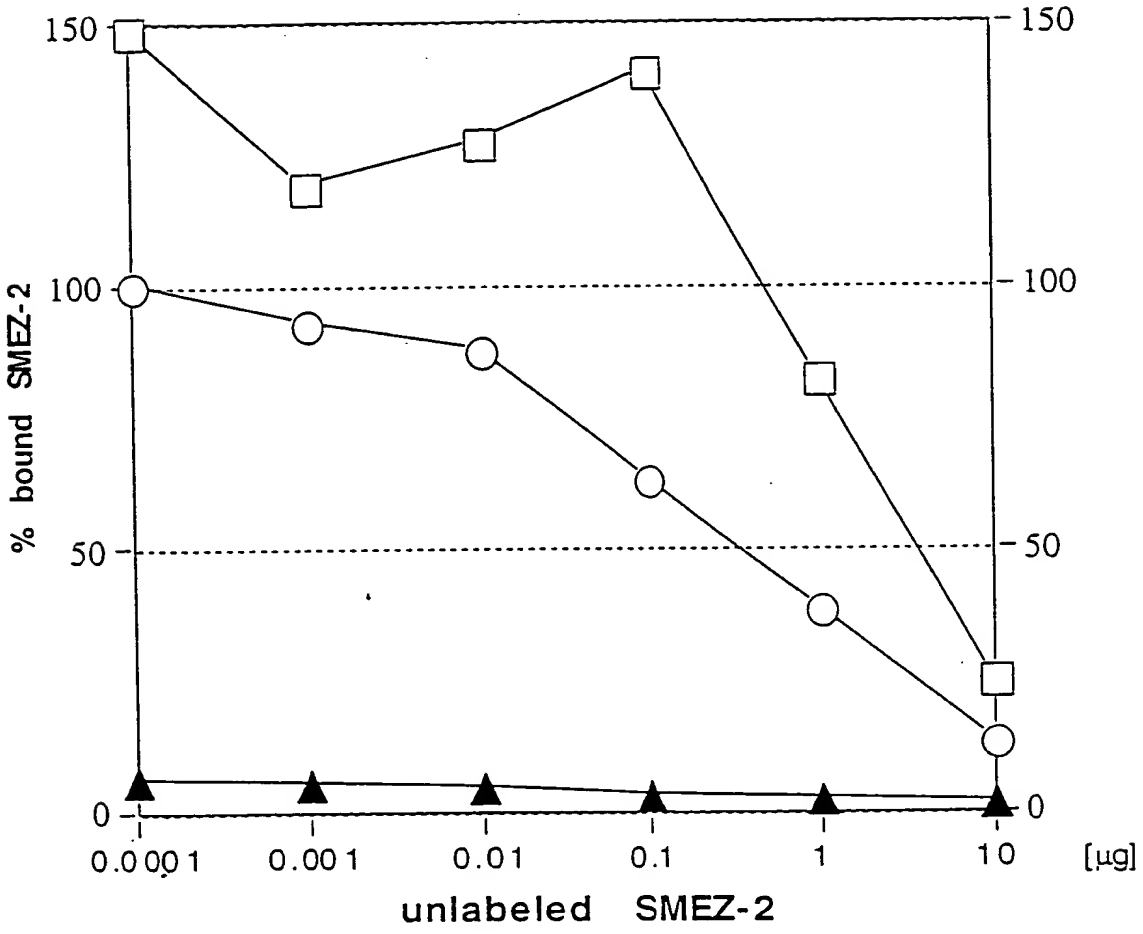
150
100
50
0
% bound SMEZ-2
0.0001
0.001
0.01
0.1
1
10
[µg]
unlabeled SMEZ-2

FIG 7

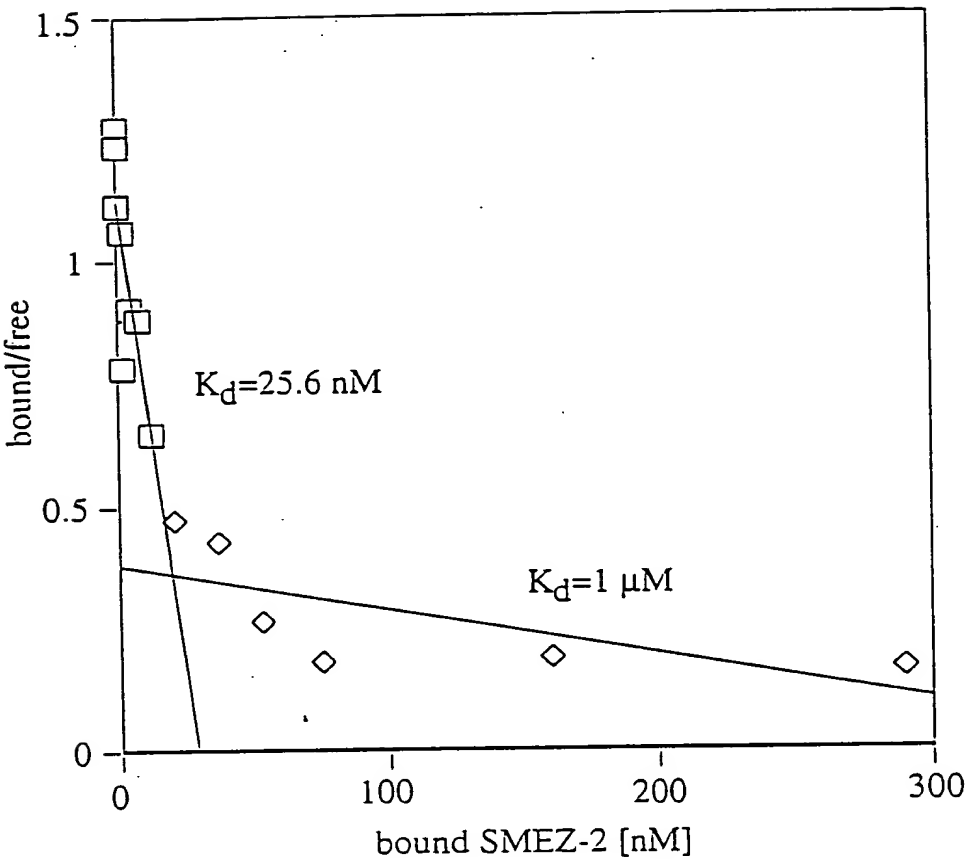

FIG 8

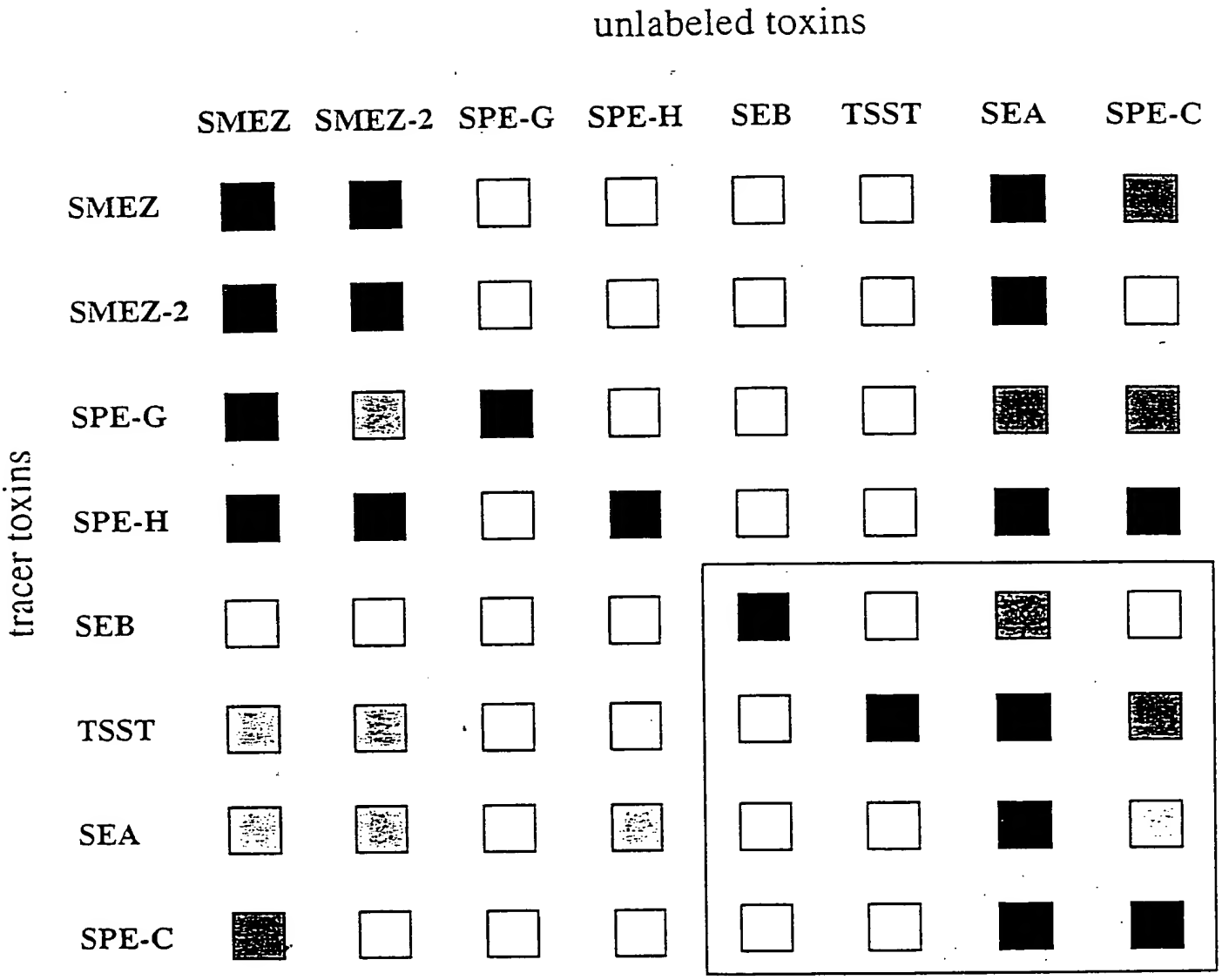
unlabeled toxins
SMEZ
SMEZ-2
SPE-G
SPE-H
SEB
TSST
SEA
SPE-C
tracer toxins
SMEZ
SMEZ-2
SPE-G
SPE-H
SEB
TSST
SEA
SPE-C

FIG 9

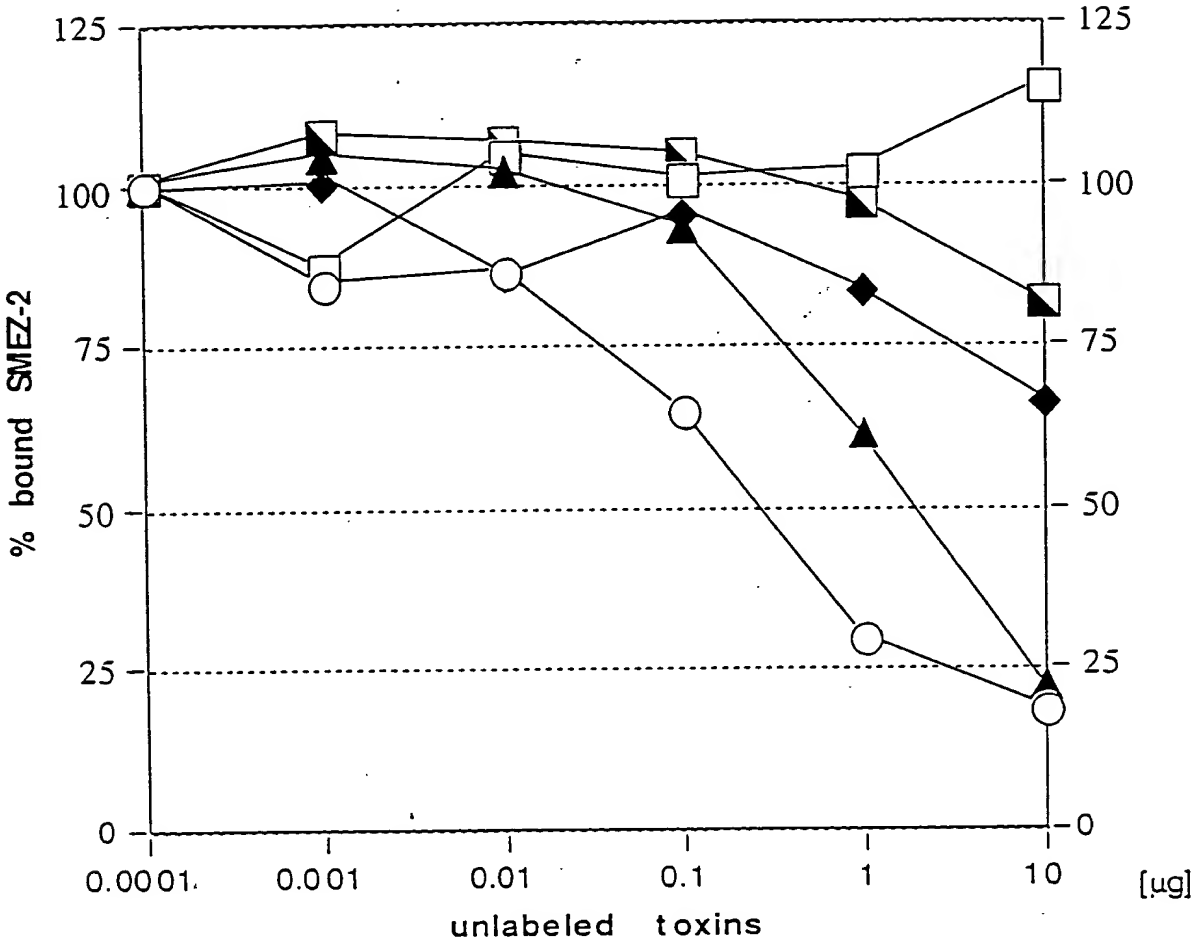
125
100
75
50
25
0
% bound SMEZ-2
0.0001
0.001
0.01
0.1
1
10
[µg]
unlabeled toxins